Springer Series on Atomic, Optical and Plasma Physics 85

Mario Capitelli · Roberto Celiberto
Gianpiero Colonna · Fabrizio Esposito
Claudine Gorse · Khaled Hassouni
Annarita Laricchiuta · Savino Longo

Fundamental Aspects of Plasma Chemical Physics

Kinetics

Springer

Springer Series on Atomic, Optical, and Plasma Physics

Volume 85

Editor-in-Chief

Gordon W.F. Drake, Windsor, Canada

Series editors

Andre D. Bandrauk, Sherbrooke, Canada
Klaus Bartschat, Des Moines, USA
Philip George Burke, Belfast, UK
Robert N. Compton, Knoxville, USA
M.R. Flannery, Atlanta, USA
Charles J. Joachain, Bruxelles, Belgium
Peter Lambropoulos, Iraklion, Greece
Gerd Leuchs, Erlangen, Germany
Pierre Meystre, Tucson, USA

The Springer Series on Atomic, Optical, and Plasma Physics covers in a comprehensive manner theory and experiment in the entire field of atoms and molecules and their interaction with electromagnetic radiation. Books in the series provide a rich source of new ideas and techniques with wide applications in fields such as chemistry, materials science, astrophysics, surface science, plasma technology, advanced optics, aeronomy, and engineering. Laser physics is a particular connecting theme that has provided much of the continuing impetus for new developments in the field. The purpose of the series is to cover the gap between standard undergraduate textbooks and the research literature with emphasis on the fundamental ideas, methods, techniques, and results in the field.

More information about this series at http://www.springer.com/series/411

Mario Capitelli • Roberto Celiberto
Gianpiero Colonna • Fabrizio Esposito
Claudine Gorse • Khaled Hassouni
Annarita Laricchiuta • Savino Longo

Fundamental Aspects of Plasma Chemical Physics

Kinetics

Springer

Mario Capitelli
University of Bari and CNR
Bari, Italy

Gianpiero Colonna
CNR
Bari, Italy

Claudine Gorse
University of Bari and CNR
Bari, Italy

Annarita Laricchiuta
CNR
Bari, Italy

Roberto Celiberto
Dipartimento di Ingegneria
Civile, Ambientale, del Territorio,
Edile e di Chimica (DICATECh)
Polytechnic of Bari
Bari, Italy

Fabrizio Esposito
CNR
Bari, Italy

Khaled Hassouni
Laboratoire des Sciences des Procédés et
des Matériaux, CNRS-INSIS
Paris, France

Savino Longo
University of Bari and CNR
Bari, Italy

ISSN 1615-5653 ISSN 2197-6791 (electronic)
Springer Series on Atomic, Optical, and Plasma Physics
ISBN 978-1-4419-8184-4 ISBN 978-1-4419-8185-1 (eBook)
DOI 10.1007/978-1-4419-8185-1

Library of Congress Control Number: 2015945655

Springer New York Heidelberg Dordrecht London
© Springer New York 2016
This work is subject to copyright. All rights are reserved by the Publisher, whether the whole or part of the material is concerned, specifically the rights of translation, reprinting, reuse of illustrations, recitation, broadcasting, reproduction on microfilms or in any other physical way, and transmission or information storage and retrieval, electronic adaptation, computer software, or by similar or dissimilar methodology now known or hereafter developed.
The use of general descriptive names, registered names, trademarks, service marks, etc. in this publication does not imply, even in the absence of a specific statement, that such names are exempt from the relevant protective laws and regulations and therefore free for general use.
The publisher, the authors and the editors are safe to assume that the advice and information in this book are believed to be true and accurate at the date of publication. Neither the publisher nor the authors or the editors give a warranty, express or implied, with respect to the material contained herein or for any errors or omissions that may have been made.

Printed on acid-free paper

Springer Science+Business Media LLC New York is part of Springer Science+Business Media (www.springer.com)

There are well-known conditions in which translational, vibrational, and rotational temperatures differ and/or various components of a system (electrons, ions, and neutral molecules, for instance) have different temperatures, and/or a system cannot be described at all using the concept of temperature (nonequilibrium, stationary, and relaxing systems). Strictly speaking, Arrhenius-type kinetics cannot be used in these cases and the ordinary expression for the rate of a chemical reaction is inapplicable.

L. Polak

Preface

In the first two books of the series *Fundamental Aspects of Plasma Chemical Physics*, we have discussed thermodynamics[1] and transport[2] of thermal plasmas characterized by equilibrium or quasi-equilibrium conditions. Plasma technology often uses working conditions very far from the equilibrium ones so that kinetic approaches are to be used to describe the properties of these plasmas. In this way we enter the scenario of *cold plasmas* which can present strong deviations from equilibrium of the internal energy distribution functions implying a loss of validity of the concept of temperature. A peculiar situation holds for electrons, which present a non-Maxwellian energy distribution function to be described by a suitable Boltzmann equation. Moreover the presence of non-Boltzmann vibrational and electronic distributions generates non-Arrhenius behavior of reaction rates, a point not easily perceived by researchers which extensively use the Arrhenius law for the relevant rates. Cold plasmas present average electron energies in the range 0.1–10 eV, while the translational temperature of heavy components ranges from room temperature to about 2,000 K. Ionization degrees well below 10^{-3} characterize this kind of plasmas which run in the torr and sub-torr pressure range even though it is nowadays possible to form atmospheric nonequilibrium plasmas. Cold plasmas are widely used in material science for cleaning, film deposition, plasma etching, surface activation, as well as to produce gas lasers (e.g., the CO_2 and excimer lasers) and negative and positive ion beams. Plasma medicine, biomaterial activation, plasma-assisted combustion, and numerous aerospace applications do extensively use cold plasmas for reaching important goals.

The present book tries to rationalize the description of cold plasmas through a chemical physics approach, in particular by using the state-to-state plasma kinetics which considers each internal state as a new species with its own cross sections.

[1]M. Capitelli, G. Colonna and A. D'Angola "Fundamental Aspects of Plasma Chemical Physics. Thermodynamics" Springer Series in Atomic, Optical and Plasma Physics (2012) Vol.66.

[2]M. Capitelli, D. Bruno and A. Laricchiuta "Fundamental Aspects of Plasma Chemical Physics. Transport" Springer Series in Atomic, Optical and Plasma Physics (2013) Vol.74.

This approach needs complete sets of state-resolved cross sections, the knowledge of which at least for the most common diatomic species (O_2, N_2, and H_2) is continuously increasing. In addition kinetic approaches based on the solution of Boltzmann equation and/or by Monte Carlo methods are being discussed especially for the description of the electron and ion energy distribution function. Coupling between electron energy distribution functions (eedf) and nonequilibrium internal (rotational, vibrational, and electronic states) distributions through second kind collisions are such to superimpose interesting structures on eedf with large consequences on plasma reactivity. This coupling should be also extended to the dissociation and ionization kinetics promoted either by electron impact or by heavy particle collisions involving excited states.

The book can be considered divided into three parts: the first part is dedicated to the dynamics of elementary processes including also heterogeneous ones and the second part to the description of plasma kinetics through the construction of suitable master equations for both atomic and molecular plasmas. Finally the third part includes different applications in applied fields such as microelectronics, fusion, and aerospace. As in the first two books of the series, some overlaps occur in the different chapters to keep part of them self-consistent allowing undergraduate and PhD students as well as researchers to construct a personal road in the understanding of the relevant topics. It is worth noting that the book can be considered complementary to other books published by one of the present authors,[3,4] on nonequilibrium plasma kinetics. An appropriate selection of the reported chapters can be used for courses on the kinetics of cold plasmas addressed to undergraduate and PhD students.

Bari, Italy

Mario Capitelli
Roberto Celiberto
Gianpiero Colonna
Fabrizio Esposito
Claudine Gorse
Khaled Hassouni
Annarita Laricchiuta
Savino Longo

[3]M. Capitelli Ed. “Non-equilibrium Vibrational Kinetics” Topics in Current Physics Springer (1986) Vol.39.

[4]M. Capitelli, B.F. Gordiets, C.M. Ferreira and A.I. Osipov “Plasma Kinetics in Atmospheric Gases” Springer Series in Atomic, Optical and Plasma Physics (1986) Vol.31.

Acknowledgments

This book is dedicated to Ettore Molinari, the founder of the plasma chemistry school in Bari, and to Gert D. Billing, Boris F. Gordiets, Aleksei I. Osipov, and Carlos Matos Ferreira for their contribution to the topics discussed in the book.

Moreover we wish to thank Giuliano D'Ammando, Paola Diomede, Vincenzo Laporta, Lucia Daniela Pietanza, Francesco Taccogna, and Massimo Tomellini for their involvement in revising the chapters (6, 8, 1, 6, 10, 3), respectively, as well as all the other Italian and international colleagues quoted in the references.

Contents

Introduction

NON EQUILIBRIUM PLASMA KINETICS is an emerging interdisciplinary discipline describing plasma conditions characterized by large deviations from the equilibrium in both the plasma components and their internal distribution functions. In particular the state-to-state description of the different components including the energy distribution functions of free electrons demands an interdisciplinary approach including quantum and classical dynamics of elementary processes, statistical mechanics and Monte Carlo particle methods ending with more or less sophisticated fluid dynamic approaches. These methods are extensively presented in the present book, which can be considered divided into three parts: the first part is dedicated to the dynamics of elementary processes and of free electrons and the second part to the description of plasma kinetics through the construction of suitable master equations for both atomic and molecular plasmas. Finally the third part includes different applications in applied fields such as microelectronics, fusion, and aerospace.

In particular Chap. 1 is dedicated to the description of electron-molecule cross sections and rates for direct and resonant processes by using semiclassical and quantum approaches. Emphasis is given to the dependence of cross sections and rates on the vibrational quantum number of the target. Particular attention is devoted to the scattering of electrons and diatomic molecules (H_2, N_2, O_2) as well as with other molecules of interest in plasma fusion. Chapter 2 reports cross sections and rates of atom-molecule interaction mainly based on QCT (Quasi Classical Trajectory) as a function of initial and final ro-vibrational quantum numbers of the target and products. Vibrational excitation rates of H-$H_2(v,j)$, N-$N_2(v)$, O-$N_2(v)$, and O-$O_2(v)$ are discussed in the whole ro-vibrational range. Chapter 3 reports the formation of nonequilibrium ro-vibrational distributions coming from heterogeneous recombination of atoms on metallic and ceramic surfaces. The results are obtained by using both quantum mechanical and kinetic approaches.

Chapter 4 introduces the reader to the solution of the Boltzmann equation by using both kinetic and Monte Carlo approaches. The two-term expansion of Boltzmann equation, which will be extensively used in the bulk of the book, is

fully described in the chapter. The Monte Carlo approach to solve the Boltzmann equation is then taken into account and also used to check the two-term expansion.

The next three chapters are dedicated to nonequilibrium plasma kinetics. In particular Chap. 5 reports several examples of coupling between excited states and eedf for different discharge and post-discharge conditions emphasizing the role of second kind (super-elastic) collisions from vibrationally and electronically excited states in structuring eedf. Chapter 6 describes in detail the collisional radiative model for atomic hydrogen under quasistationary, stationary, and time-dependent situations. The first part of this chapter uses a Maxwell distribution function for free electrons, while the second part uses non-Boltzmann eedf especially for recombining plasma situations. In the same chapter, we discuss the dependence of excitation and ionization cross sections on the principal quantum number of atomic hydrogen. Chapter 7 describes in detail the nonequilibrium vibrational kinetics of diatomic molecules emphasizing the redistribution of vibrational quanta, introduced by different interactions, by VV (vibration-vibration) and VT (vibration-translation) energy exchange transfer processes.

The third part of the book deals with the applications. Chapter 8 discusses parallel plate RF reactors for microelectronics applications by using a self-consistent PIC (Particle in Cell) model able to yield eedf and vibrational distributions as a function of the distance of electrodes. In the same chapter, we report nonequilibrium translational distributions of ions derived by collisional sheath dynamics. Chapter 9 describes in detail the nonequilibrium vibrational kinetics of nitrogen discharges emphasizing in particular the possibility of vibrational mechanisms in affecting the dissociation rates of nitrogen. Chapter 10 reports the kinetics of negative ion H^- sources under different plasma configurations (multipole magnetic plasma, RF discharges) to be used for injecting intense neutral beams in tokamak facilities for fusion. Emphasis is given to the collisional production of negative H^- ions either through the dissociative attachment from vibrationally excited molecules or through dissociative attachment for Rydberg states, and Chap. 11 is dedicated to the description of the plasma kinetics during nozzle expansion and shock wave interaction for miming conditions met under reentry conditions for aerospace applications. Under these conditions we recover eedf and vdf very far from Maxwell and Boltzmann distributions.

Finally Chap. 12 considers the challenge of properly accounting the vibrational issue in the kinetics of polyatomic molecules, as CO_2 plasmas, nowadays collecting a large interest in the community for their relevance to technological applications in the fields of energy and environment.

Chapter 1
Electron-Molecule Collision Cross Sections and Rate Coefficients for Processes Involving Excited States

The formulation of a theoretical model for non-equilibrium plasmas relies primarily on the knowledge of cross section information on collisional processes involving excited species. This is particularly true for molecular plasmas where the presence of molecules, characterized by a large spectrum of rovibronic states, gives rise to an enormous number of scattering processes where momentum or energy transfers, as well as reactive events, can occur. This implies, then, the determination of the corresponding cross sections for each process and for a suitable range of relative kinetic energy of the collision partners, which results in the need of large cross section databases.

A first example of low-temperature non-equilibrium molecular plasma is provided, in space explorations, by the atmospheric gases interacting with the thermal shield of a space vehicle during the immersion in the atmosphere of a planet at hypersonic speed (re-entry conditions). The energy exchanges, consequent to the shock wave generated in the impact, induce the formation of a molecular plasma in thermal and chemical non-equilibrium conditions, characterized by a non-Boltzmann population of the internal states. Then redistribution of energy takes place through a complex collision physics where a role of primary importance is played by the electron-molecule collisions (Capitelli et al. 2009).

Hydrogen/deuterium plasmas in fusion technology offer a second relevant example of a non-equilibrium systems. Here the hydrogen, used for the nuclear energy production, getting into the low-temperature regions of the containing vessel (edge and divertor plasmas) condenses in H_2 excited molecules which play a role of capital importance in affecting the performance of the nuclear devices (Clark and Reiter 2005; Capitelli et al. 2006).

This Chapter deals with internal transitions, induced by electron impact, of diatomic molecules initially in a given quantum state, with particular emphasis on the vibrational excitations, which play a prominent role in the energy balance of the molecular plasmas (Capitelli et al. 2011). An efficient process for the activation of the vibrational degrees of freedom is represented by the resonant collisions whose

© Springer New York 2016

M. Capitelli et al., *Fundamental Aspects of Plasma Chemical Physics*, Springer Series on Atomic, Optical, and Plasma Physics 85, DOI 10.1007/978-1-4419-8185-1_1

mechanism involves the capture from the molecule of the incident electron, with the concomitant formation of a molecular anion. This is a transient species, better described as a resonant state, which can either decay, by electron emission, back into some excited vibrational level of the neutral molecule, giving rise to the so-called resonant vibrational excitation (RVE), or can dissociate by production of a neutral atom and a negative atomic ion. This last process, known as dissociative electron attachment (DEA), can occur if the atomic negative ion exists in a stable state. Unlike the *direct* inelastic vibrational excitation, which is an inefficient process usually involving few vibrational levels, particularly for homonuclear molecules owing no permanent dipole moment, multi-quantum vibrational transitions can occur, on the contrary, through the above resonant mechanism which can promote effectively the activation of high vibrational levels.

Hence the importance of reliable information on the corresponding state-to-state cross sections in the construction of realistic models of molecular plasmas. Beside the laboratory measurements, which can provide precious cross section information on electron-impact vibrational excitation, at least for those levels experimentally accessible, cross section calculations can be performed with no particular limitations, being the theoretical description of the resonant collisions within the range of the present state-of-the-art of the scattering theories. So complete sets of cross sections for electron-impact processes, involving all the vibrational levels of a given molecule, can be obtained.

One of the outcomes of a modeling in molecular plasma is the electron energy distribution function (eedf) which can be strongly affected, beside the other processes, by the electron collisions with vibrationally excited molecules, so that, in stationary conditions, the eedf can significantly deviate from the Maxwellian distribution (see Chaps. 5 and 9–11). Maxwellian state-specific rate coefficients are in any case helpful to model the dependence on the vibrational quantum number in equilibrium plasmas.

In the next section we will formulate the resonance theory for electron-molecule collision cross section calculations for both RVE and DEA processes, while in the subsequent sections we will review the main results pertinent for molecular plasmas in aerospace and fusion applications.

1.1 Theoretical Model of Resonant Collisions

When a diatomic molecule, M_2, in its ground electronic state, X, and in a given ro-vibrational level, denoted by (J_i, v_i), interacts with an electron of incident energy ϵ_i, the following processes can occur (Bardsley and Mandl 1968):

$$M_2(X, J_i, v_i) + e(\epsilon_i) \rightarrow M_2^- \rightarrow M_2(X, J_f, v_f) + e(\epsilon_f) \qquad \text{(RVE)} \qquad (1.1)$$

$$M_2(X, J_i, v_i) + e(\epsilon_i) \rightarrow M_2^- \rightarrow M + M^- \qquad \text{(DEA)} \qquad (1.2)$$

where (J_f, v_f) denotes a final ro-vibrational level and ϵ_f the kinetic energy of the outgoing electron. The first process leads to a ro-vibrational excitation and the second to dissociation. In both cases a resonant state of the M_2^- molecular ion is formed after the trapping of the incident electron within the target molecule M_2. RVE includes also the excitation to the vibrational continuum of the neutral molecule, followed by dissociation, according to the process

$$M_2(X, J_i, v_i) + e(\epsilon_i) \rightarrow M_2^- \rightarrow M + M + e(\epsilon_f) \tag{1.3}$$

This channel (Laporta et al. 2014, 2015) will not be considered in the present Chapter.

The theoretical description of the resonant collision process starts from the Schrödinger equation,

$$H\Psi(\mathbf{r}_M, \mathbf{r}_e, \mathbf{R}) = [H_{el} + T_N]\, \Psi(\mathbf{r}_M, \mathbf{r}_e, \mathbf{R}) = E\, \Psi(\mathbf{r}_M, \mathbf{r}_e, \mathbf{R}), \tag{1.4}$$

where the Hamiltonian operator H is expressed as a sum of the electronic Hamiltonian, H_{el}, and the nuclear operator T_N. Ψ is the wave function for the $M_2 + e$ scattering system depending on the target electron coordinates, denoted collectively with $\mathbf{r}_M$, on the incident electron vector position $\mathbf{r}_e$, and on the internuclear distance vector $\mathbf{R}$. E is the total energy. The solution of Eq. (1.4) can be searched by resorting to a standard treatment where the scattering wave function is expressed in terms of a close-coupling expansion, including bound and continuum states. The orthonormal basis set is formed by wave functions factorized, according to the Born-Oppenheimer approximation, in an electronic and nuclear part. In the applications a simplified model is usually adopted where only one discrete electronic state is selected, which can be written as $\Phi(\mathbf{r}_M, \mathbf{r}_e; R)\xi(\mathbf{R})$. Here Φ is the electronic eigenfunction of the Hamiltonian H_{el}, depending on the electron coordinates and, parametrically, on the internuclear distance R, while $\xi(\mathbf{R})$ is the resonant nuclear wave function. No limitations, instead, are imposed to the continuum spectrum whose expansion can be written in terms of the product $\Psi_\epsilon^n(\mathbf{r}_M, \mathbf{r}_e; R)\chi_v^n(\mathbf{R})$, where Ψ_ϵ^n is the wave function for the electronic state n, depending on the continuum energy ϵ, and $\chi_v^n(\mathbf{R})$ is the nuclear wave function of the target molecule, where $v = (J, v)$ denotes the ro-vibrational quantum numbers. These wave functions are solution of the target nuclear equation given by

$$\left[T_N + V_M^n(R) - E_v^n\right] \chi_v^n(\mathbf{R}) = 0, \tag{1.5}$$

where $V_M^n(R)$ is the potential energy of the electronic state of the neutral molecule and E_v^n the associated ro-vibrational eigenvalues. Thus the scattering wave function is written as (Wadehra 1986),

$$\Psi(\mathbf{r}_M, \mathbf{r}_e, \mathbf{R}) \approx \Phi(\mathbf{r}_M, \mathbf{r}_e; R)\xi(\mathbf{R}) + \sum_{n,v} \int d\epsilon f_v^n(\epsilon) \Psi_\epsilon^n(\mathbf{r}_M, \mathbf{r}_e; R) \chi_v^n(\mathbf{R}) \tag{1.6}$$

where $f_\nu^n(\epsilon)$ is a linear combination coefficient and the electronic wave functions are assumed antisymmetrized. Equation (1.6) obeys to the boundary condition:

$$\begin{aligned}\Psi(r_e \to \infty) \longrightarrow\ & e^{i\mathbf{k}_{\nu_i}^{n_i}(\epsilon_i)\cdot\mathbf{r}_e}\Psi^{n_i}(\mathbf{r}_M;R)\chi_{\nu_i}^{n_i}(\mathbf{R}) + \\ & + \sum_{n,\nu}\Psi^n(\mathbf{r}_M;R)\chi_\nu^n(\mathbf{R})\int d\epsilon f_\nu^n(\epsilon)e^{i\mathbf{k}_\nu^n(\epsilon)\cdot\mathbf{r}_e} = \\ & = \sum_{n,\nu}\Psi^n\chi_\nu^n\int d\epsilon\left[\delta(\epsilon-\epsilon_i)\delta_{nn_i}\delta_{\nu\nu_i} + f_\nu^n(\epsilon)\right]e^{i\mathbf{k}_\nu^n(\epsilon)\cdot\mathbf{r}_e} \qquad (1.7)\end{aligned}$$

where the index i denotes the initial state of the system. $k(\epsilon) = (2m\epsilon/\hbar)^{1/2}$ is the momentum of the free electron. m is the electron mass and $\hbar$ the Dirac constant. $\Psi^n(\mathbf{r}_M;R)$ is the target electronic wave function. In the last line we have shortened the notation by including the first term under the sum-integral and omitted the arguments in the wave functions. In writing Eq. (1.7) we have used the fact that $\Phi(r_e \to \infty) = 0$ due to the bound nature of the discrete wave function. From the last line of Eq. (1.7) it is immediate to deduce:

$$f_{\nu_i}^{n_i}(\epsilon_i) = \delta(\epsilon-\epsilon_i)\delta_{nn_i}\delta_{\nu\nu_i}. \qquad (1.8)$$

Inserting now the expansion (1.6) in Eq. (1.4), and assuming, according to the fixed-nuclei approximation, $\mathrm{T}_N\Phi = \mathrm{T}_N\Psi_\epsilon^n \approx 0$, we obtain:

$$\begin{aligned}& \xi(\mathbf{R})\mathrm{H}_{el}\Phi(\mathbf{r}_M,\mathbf{r}_e;R) + \Phi(\mathbf{r}_M,\mathbf{r}_e;R)\mathrm{T}_N\xi(\mathbf{R}) + \\ & \quad + \sum\!\!\!\!\!\!\int_{n,\nu} d\epsilon f_\nu^n(\epsilon)\chi_\nu^n(\mathbf{R})\mathrm{H}_{el}\Psi_\epsilon^n(\mathbf{r}_M,\mathbf{r}_e;R) + \\ & \quad + \sum\!\!\!\!\!\!\int_{n,\nu} d\epsilon f_\nu^n(\epsilon)\Psi_\epsilon^n(\mathbf{r}_M,\mathbf{r}_e;R)\mathrm{T}_N\chi_\nu^n(\mathbf{R}) = \\ & = E\left[\Phi(\mathbf{r}_M,\mathbf{r}_e;R)\xi(\mathbf{R}) + \sum\!\!\!\!\!\!\int_{n,\nu} d\epsilon f_\nu^n(\epsilon)\Psi_\epsilon^n(\mathbf{r}_M,\mathbf{r}_e;R)\chi_\nu^n(\mathbf{R})\right]. \qquad (1.9)\end{aligned}$$

Multiplying now this equation on the left by $\int d\mathbf{r}_M d\mathbf{r}_e \Phi^*(\mathbf{r}_M,\mathbf{r}_e;R)$ and using the orthonormality of the basis set, we get finally:

$$\left[\mathrm{T}_N + \mathrm{V}^-(R) - \mathrm{E}\right]\xi(\mathbf{R}) = -\sum_{n,\nu}\chi_\nu^n(\mathbf{R})\int d\epsilon f_\nu^n(\epsilon)V_{dc}^n(\epsilon;R), \qquad (1.10)$$

where $\mathrm{V}^-(R) = \langle\Phi|\mathrm{H}_{el}|\Phi\rangle$ is the *adiabatic* potential energy of the bound electronic state of M_2^- molecular ion. Equation (1.10) shows the role of the *discrete-continuum coupling matrix* element $\mathrm{V}_{dc}^n(\epsilon;R) = \langle\Phi|\mathrm{H}_{el}|\Psi_\epsilon^n\rangle$. This describes the interaction

between the discrete and continuum spectrum of the $M_2 + e$ system and determines the existence of the resonance. If the bound-continuum coupling is weak, in fact, the right-hand side of Eq. (1.10) becomes negligibly small, so that the whole expression reduces to the nuclear Schrödinger equation of a non-resonant stable state of the M_2^- molecular ion, where E and $\xi(\mathbf{R})$ are now its stable ro-vibrational eigenvalue and eigenfunction respectively.

The coefficient $f_\nu^n(\epsilon)$ also depends on the coupling matrix. It can be found by premultiplying Eq. (1.9) by $\int d\mathbf{R} d\mathbf{r}_M d\mathbf{r}_e \Psi_{\epsilon'}^{n'*}(\mathbf{r}_M, \mathbf{r}_e; R)\chi_{\nu'}^{n'*}(\mathbf{R})$. One has:

$$f_\nu^n(\epsilon) = \lim_{\eta\to 0} \int d\mathbf{R}\chi_\nu^{n*}(\mathbf{R}) \frac{\mathrm{V}_{dc}^{n*}(\epsilon, R)}{\mathrm{E} - \mathrm{E}_\nu^n - \epsilon + i\eta} \xi(\mathbf{R}) + \delta(\epsilon - \epsilon_i)\delta_{nn_i}\delta_{\nu\nu_i}, \tag{1.11}$$

where we have suppressed the prime superscript and added the last term on the right coming from Eq. (1.8). Using Eq. (1.11) in Eq. (1.10) we have:

$$[\mathrm{T}_N + \mathrm{V}^-(R) - \mathrm{E}]\,\xi(\mathbf{R}) = -\mathrm{V}_{dc}^{n_i}(\epsilon_i, R)\chi_{\nu_i}^{n_i}(\mathbf{R}) - \int d\mathbf{R}' K(\mathbf{R}, \mathbf{R}')\xi(\mathbf{R}') \tag{1.12}$$

where

$$K(\mathbf{R}, \mathbf{R}') = \sum_{n,\nu} \chi_\nu^{n*}(\mathbf{R}')\chi_\nu^n(\mathbf{R}) \left[\Delta_\nu^n(R', R, \mathrm{E} - \mathrm{E}_\nu^n) - \frac{i}{2}\Gamma_\nu^n(R', R, \mathrm{E} - \mathrm{E}_\nu^n)\right]. \tag{1.13}$$

The *level shift*, Δ_ν^n, and the *resonance width*, Γ_ν^n, are defined by:

$$\Delta_\nu^n(R, R', \mathrm{E} - \mathrm{E}_\nu^n) = P \int_0^\infty d\epsilon \frac{1}{2\pi} \frac{\Gamma_\nu^n(R, R', \mathrm{E} - \mathrm{E}_\nu^n)}{\mathrm{E} - \mathrm{E}_\nu^n - \epsilon}, \tag{1.14}$$

where P denotes the principal value of the integral and

$$\Gamma_\nu^n(R', R, \mathrm{E} - \mathrm{E}_\nu^n) = 2\pi \mathrm{V}_{dc}^{n*}(\mathrm{E} - \mathrm{E}_\nu^n, R')\mathrm{V}_{dc}^n(\mathrm{E} - \mathrm{E}_\nu^n, R). \tag{1.15}$$

Equation (1.12) is usually referred to as the *non-local form* of the resonant nuclear equation. This denomination comes form the fact the value in a given point $\mathbf{R}$ of the unknown function $\xi(\mathbf{R})$ on the left-hand side, depends on the values of the same function in the whole range of the integration variable, $\mathbf{R}'$, on the right. In this form the non-local coupling matrix elements, $\mathrm{V}_{dc}^n(\mathrm{E} - \mathrm{E}_\nu^n, R)$, are function of both the internuclear distance R and the energy $\mathrm{E} - \mathrm{E}_\nu^n$. The lack of information in literature on these non-local quantities for many molecules of applicative interest, and also the need of the production of large cross section databases, which imposes fast computational methods, can make convenient the use of a *local* approximate form of Eq. (1.12). This can be obtained if we assume that the quantity in the square bracket in Eq. (1.13) can be considered as independent of the ro-vibrational levels ν. This is true for example when $\mathrm{E} \gg \mathrm{E}_\nu^n$, so that the level shift and the width become a weak function of E_ν^n. In this conditions, instead to suppress the eigenvalue E_ν^n, it can

be replaced by a constant value opportunely selected. Assuming then $\mathrm{E}_{\nu}^{n} \approx \mathrm{E}_{\bar{\nu}}^{n}$, and putting $\mathrm{E} - \mathrm{E}_{\bar{\nu}}^{n} \approx \bar{\epsilon}$, Eq. (1.13) can be rewritten as:

$$K(\mathbf{R}, \mathbf{R}') \approx \sum_{n} \left[\Delta_{\bar{\nu}}^{n}(R', R, \bar{\epsilon}) - \frac{i}{2} \Gamma_{\bar{\nu}}^{n}(R', R, \bar{\epsilon}) \right] \times$$

$$\times \sum_{\nu} \chi_{\nu}^{n*}(\mathbf{R}') \chi_{\nu}^{n}(\mathbf{R}) =$$

$$= \sum_{n} \left[\Delta_{\bar{\nu}}^{n}(R', R, \bar{\epsilon}) - \frac{i}{2} \Gamma_{\bar{\nu}}^{n}(R', R, \bar{\epsilon}) \right] \delta_{n}(R - R'), \tag{1.16}$$

where we have used the completeness of the ro-vibrational basis set. Inserting this approximate form of the kernel $K(\mathbf{R}, \mathbf{R}')$ in Eq. (1.12), and using the $\delta-$function properties in the right-hand side integration, we get the local resonant nuclear equation,

$$\left[\mathrm{T}_{N} + \mathrm{V}^{-}(R) + \Delta_{tot}(R) - \frac{i}{2} \Gamma_{tot}(R) - \mathrm{E} \right] \xi(\mathbf{R}) = -\mathrm{V}_{dc}^{n_i}(\epsilon_i, R) \chi_{\nu_i}^{n_i}(\mathbf{R}), \tag{1.17}$$

where for brevity we have put,

$$\Delta_{tot} = \sum_{n} \Delta_{\bar{\nu}}^{n}(R), \qquad \Gamma_{tot} = \sum_{n} \Gamma_{\bar{\nu}}^{n}(R). \tag{1.18}$$

The complex quantity in Eq. (1.17), $\mathrm{V}^{-} + \Delta_{tot} - i\Gamma_{tot}/2$, is known as *optical potential*.

The last step for the solution of Eq. (1.17) is the expansion of both $\xi(\mathbf{R})$ and $\chi_{\nu_i}^{n_i}(\mathbf{R})$ in terms of spherical harmonics where $\xi(R)/R$ and $\chi_{\nu_i}^{n_i}(R)/R$ are the radial parts. After some manipulation (Wadehra 1986) the final local form for the radial equation is obtained,

$$\left[\mathrm{T}_{N} + \mathrm{V}^{-}(R) + \Delta_{tot}(R) - \frac{i}{2} \Gamma_{tot}(R) - \mathrm{E} \right] \xi(R) = -\mathrm{V}_{dc}^{n_i}(\epsilon_i, R) \chi_{\nu_i}^{n_i}(R). \tag{1.19}$$

This is the equation used for cross section calculations discussed in next sections and will be referred to as the *local complex-potential* (LCP) approximation. Once this equation is solved, with the appropriate boundary conditions for $\xi(R)$, the cross sections for DEA and RVE can be calculated (Wadehra 1986).

The widths can be obtained from the local form of Eq. (1.15) as $\Gamma_{\bar{\nu}}^{n}(\bar{\epsilon}; R) = 2\pi \left| \mathrm{V}_{dc}^{n}(\bar{\epsilon}; R) \right|^{2}$. The input quantities for solving Eq. (1.19) are then represented by the adiabatic potential $\mathrm{V}^{-}(R)$, the coupling matrix elements $\mathrm{V}_{dc}^{n}(\bar{\epsilon}; R)$ and the initial electronic state potential $\mathrm{V}_{M}^{n_i}(R)$ of the neutral molecule, which allows for the calculation of ro-vibrational eigenvalues and eigenfunctions through Eq. (1.5). The total scattering energy is then expressed as $\mathrm{E} = \mathrm{E}_{\nu_i}^{n_i} + \epsilon_i$.

1.2 Resonant Collisions Involving Atmospheric Molecules

When a spacecraft, after a space mission, returns back to the Earth, its thermal shield interacts with the terrestrial atmosphere. The modeling of the plasma created at the vehicle surface requires cross sections and rate coefficients for the collision processes involving N_2 and O_2 molecules, which are the main components of the atmospheric gas, as well as those for other molecular species like NO, CO, CO_2 present in small fractions. In planetary explorations, however, also the atmospheres of other planets, with their own compositions, must be considered. Relevant examples are the Venus and Mars atmospheres, which consist mostly of CO and CO_2 species, or the gaseous giant planets, like Jupiter or Saturn, where hydrogen is the most abundant constituent.

In this section we will review the resonant vibrational excitation cross sections and rate coefficients calculated in our group, relevant for atmospheric modeling, for electron-collision processes involving the above molecules in excited vibrational levels (Laporta et al. 2012a,b, 2013, 2014; Celiberto et al. 2014). A special place is occupied by hydrogen because of its importance also in nuclear energy researches, and will be discussed in this Chapter in connection with fusion technology.

1.2.1 N_2, O_2 *and* NO *Molecules*

Resonant vibrational cross sections (RVE) have been calculated for the process (Laporta et al. 2012b, 2014):

$$N_2(X\,^1\Sigma_g^+, v_i) + e \rightarrow N_2^-(X\,^2\Pi_g) \rightarrow N_2(X\,^1\Sigma_g^+, v_f) + e, \tag{1.20}$$

Recent calculations for the above process were performed in Laporta et al. (2014) by using an accurate potential curve for the ground state $N_2(X\,^1\Sigma_g^+)$ (Le Roy et al. 2006), while that of the $N_2^-(X\,^2\Pi_g)$ state were obtained by ab initio calculations using the R-matrix method, which provided also the resonance width. The obtained results are shown in Fig. 1.1.

The RVE cross sections have been calculated for all the possible transitions $v_i \rightarrow v_f$ linking the 59 vibrational levels supported by the N_2 ground state potential curve (Laporta et al. 2014). Figure 1.2 shows a comparison with the experiments (Allan 1985) for the transitions $0 \rightarrow 1, 5, 10$. Quite satisfactory is the agreement theory-experiment for the $0 \rightarrow 1$ and $0 \rightarrow 5$ transitions, while some discrepancy arises for the $0 \rightarrow 10$ excitation, probably due to the very small absolute cross section values which implies a reduced accuracy. However, for large multi-quantum excitations we can expect that the LCP approximation is no longer valid so that a non-local treatment of the dynamical model could be more appropriate (Cederbaum and Domcke 1981).

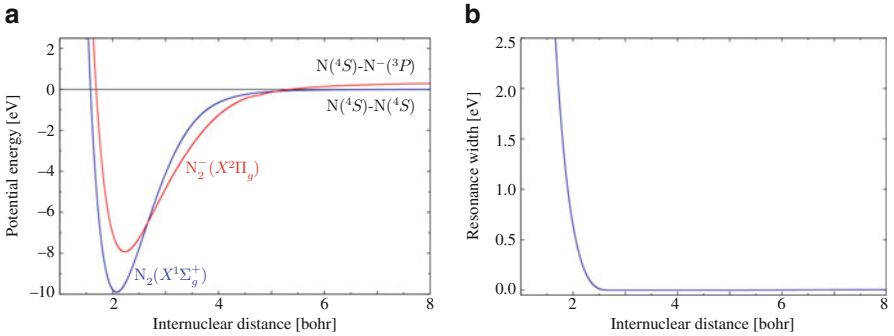

Fig. 1.1 (**a**) Potential curves for $N_2(X\,^1\Sigma_g^+)$ and $N_2^-(X\,^2\Pi_g)$ states and (**b**) the resonance width (Laporta et al. 2014)

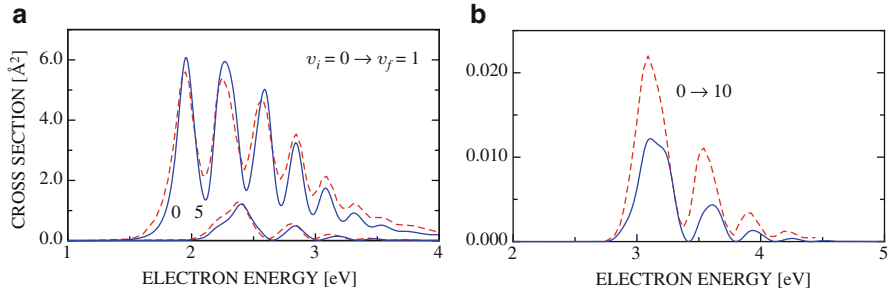

Fig. 1.2 Comparison of the theoretical cross sections (Laporta et al. 2014) (*full-blue line*) with the experiments (Allan 1985) (*dashed-red lines*) for the transitions shown in the panels

Very good agreement is instead observed in Fig. 1.3 where the theoretical cross sections are compared with the experimental results of Wong, as reported by Dubé and Herzenberg (1979), for the $0 \rightarrow 1$ and $0 \rightarrow 2$ transitions. A comparison of the cross sections calculated by the LCP approximation with the R-matrix results is shown in Fig. 1.4. A shift in the peak positions is observed in this case, probably determined by the different input parameters used in the two calculations.

Figure 1.5a, b show elastic and inelastic RVE cross sections for some transitions as a function of the incident electron energy. The oscillating structures observed in all the curves, follow mainly the behavior of the bound vibrational wave functions of $N_2^-(X\,^2\Pi_g)$ ion and disappear in the continuum region above the dissociation limit of the resonant state (Celiberto et al. 2013b). Figure 1.5c, d show the corresponding rate coefficients, calculated by assuming a Maxwellian electron energy distribution function and found in good agreement with previous calculations (Laporta et al. 2012b; Huo et al. 1986, 1987).

The RVE collisions involving the oxygen molecule can be written as:

$$e + O_2(X\,^3\Sigma_g^-, v_i = 0-41) \rightarrow O_2^-(^2\Pi_g, ^2\Pi_u, ^4\Sigma_u^-, ^2\Sigma_u^-) \rightarrow$$
$$\rightarrow e + O_2(X\,^3\Sigma_g^-, v_f = 0-41) \qquad (1.21)$$

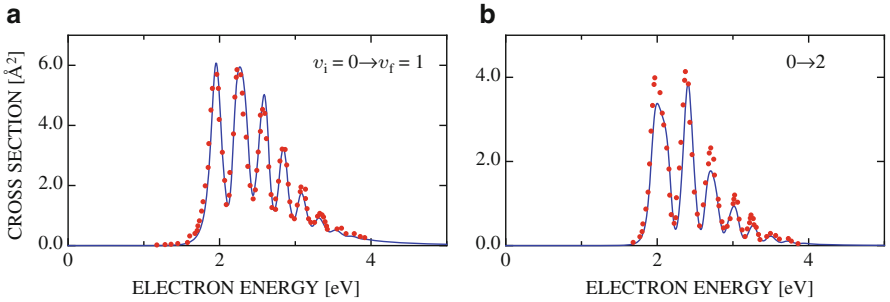

Fig. 1.3 Comparison of the theoretical cross sections (Laporta et al. 2014) (*full-blue line*) with the experiments of Wong, as cited by Dubé and Herzenberg (1979) (*markers*), for the transitions shown in the panels

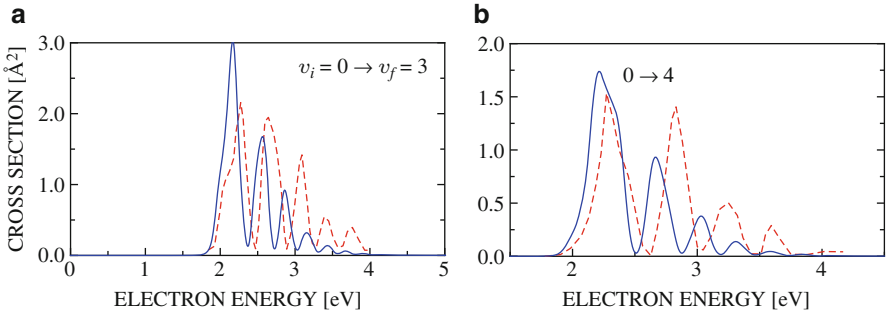

Fig. 1.4 Comparison of the theoretical cross sections calculated by the LCP model (Laporta et al. 2014) (*full-blue line*) and the R-matrix method (Schneider et al. 1979) (*dashed-red lines*) for the transitions shown in the panels

where four resonant states are implicated in the process. The potential curves for the O_2 and O_2^- electronic states were obtained by using the MOLPRO chemistry code (Werner et al. 2010) and by exploiting existing data in literature. Details of the calculations are given elsewhere (Laporta et al. 2013) and the results are shown in Fig. 1.6. Forty two vibrational levels, belonging to the ground electronic state of the neutral molecule were found, and cross sections and rates were calculated for all transitions. A comparison of the theoretical calculations with the experiments is shown in Fig. 1.7. A good agreement is observed between the LCP calculations (Laporta et al. 2013) with the experimental results (Noble et al. 1996) for the $0 \rightarrow 1, 2$ transitions, while some discrepancy is observed with the R-matrix results (Noble et al. 1996), for the $0 \rightarrow 1, 2, 3, 4$ excitations, probably due to the fact that these last calculations included the $^4\Sigma_u^-$ resonance only. A little worse is the comparison with the experiments for the $0 \rightarrow 3, 4$ transitions, where the LCP calculations show larger cross sections. We should stress here the fact that the experimental cross sections shown in Fig. 1.7, were obtained from the measured differential cross sections by assuming for the incident electron a pure p-wave

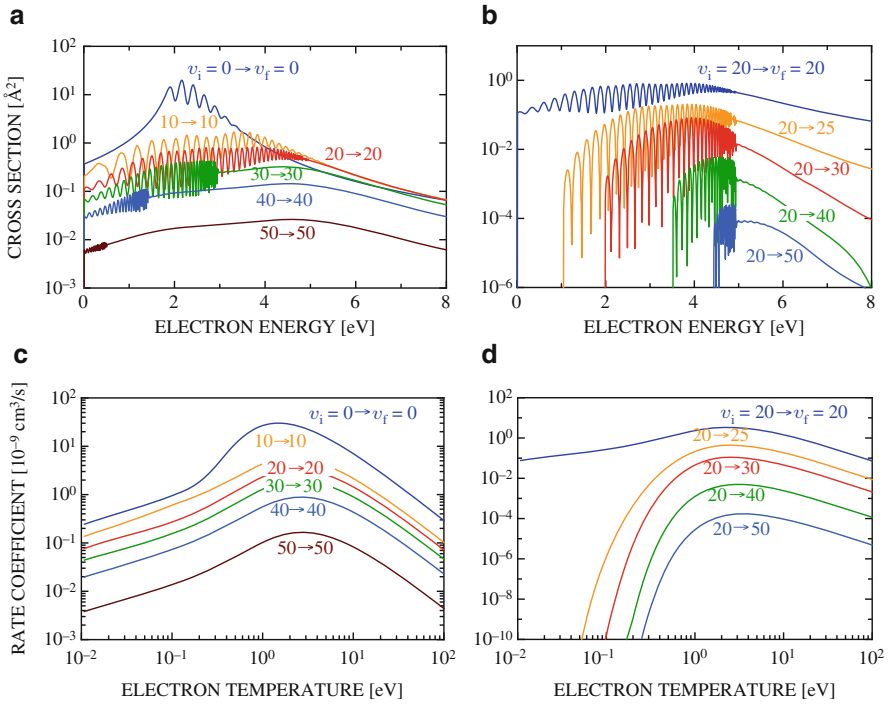

Fig. 1.5 Electron-N_2 elastic (**a**) and inelastic (**b**) cross sections and the corresponding rate coefficients (**c**)–(**d**), for the transitions shown in the panels

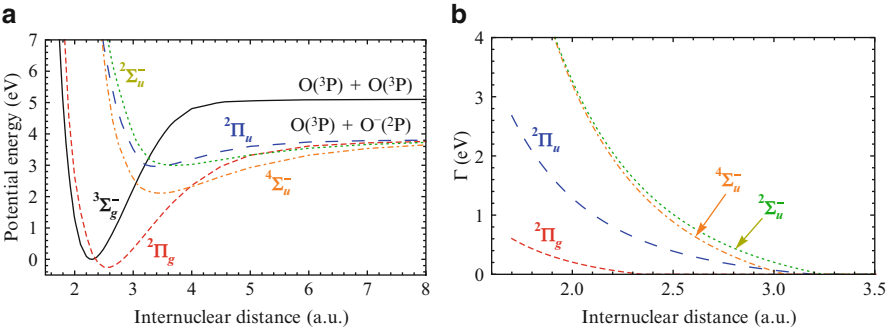

Fig. 1.6 (**a**) Potential curves for the O_2 ground state and for the four O_2^- resonant states as shown in the figure. (**b**) The corresponding resonance widths

behavior ($l = 1$) while, according to the analysis of Allan (1995), a d-wave ($l = 2$) contribution should be considered (Laporta et al. 2013).

Cross sections and rate coefficients for some transitions are shown in Fig. 1.8. The different features exhibited by the cross sections in different range of electron energies, are determined by the different contributions coming from the four

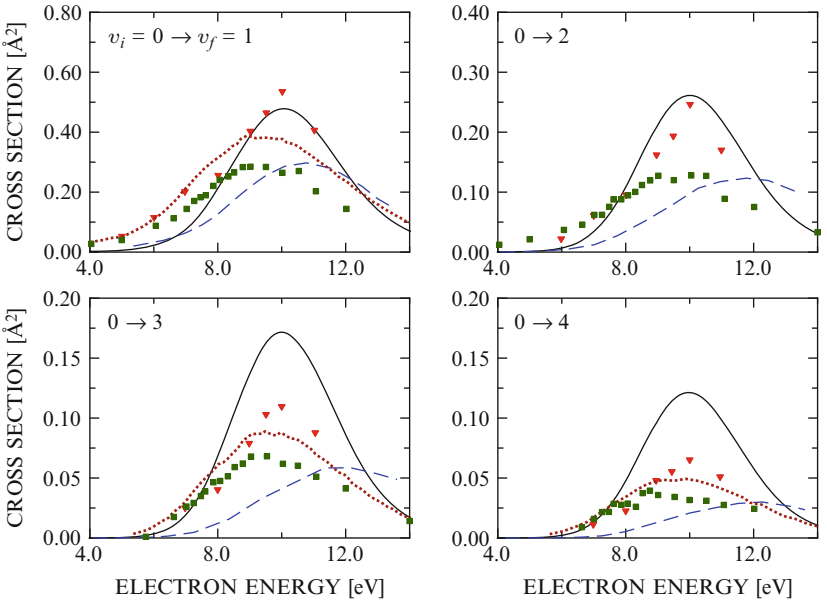

Fig. 1.7 Comparison of calculated and measured RVE cross sections in e-O_2 collisions. Theoretical: *solid lines* (Laporta et al. 2013), *long-dashed lines* (Noble et al. 1996). Experimental: *triangles* (Noble et al. 1996), *squares* (Wong et al. 1973) and *dotted lines* (Allan 1995)

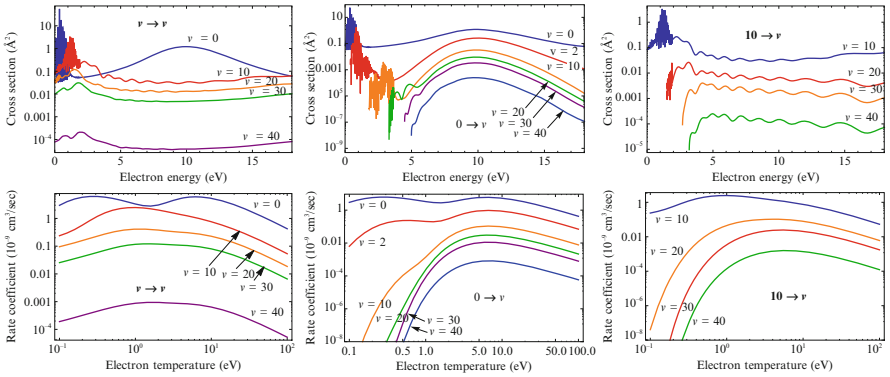

Fig. 1.8 Electron-O_2 elastic and inelastic cross sections (*upper panels*) and the corresponding rate coefficients (*lower panels*), for the shown transitions

resonant states. The rapid oscillations, in fact, observed at very low energies (<4 eV) comes from the dominance of the $^2\Pi_g$ symmetry (see Fig. 1.6a), while at larger energy (∼10 eV) the $^4\Sigma_u^-$ gives the main contribution. The structures present in the $10 \rightarrow v'$ transitions, as well as those for the $v \rightarrow v$ case for large v, are probably due to the overlap of the vibrational wave functions of the O_2 molecule with the continuum of the O_2^- resonant states (Laporta et al. 2013).

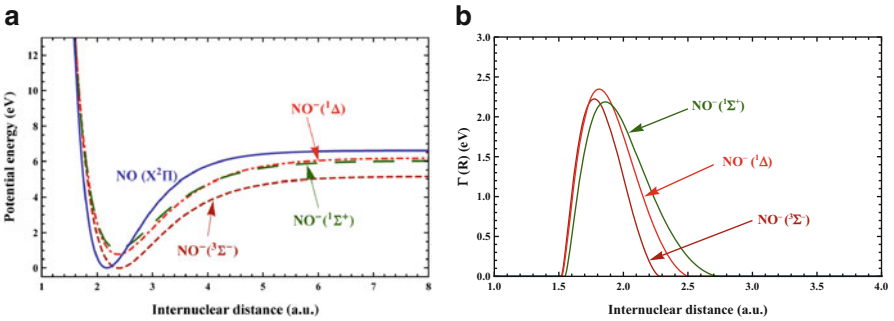

Fig. 1.9 (**a**) Potential curves for the NO ground state and for the three NO^- resonant states as shown in the figure. (**b**) The corresponding resonance widths

Dissociative electron attachment cross sections were also calculated for O_2 molecule, along with those for the resonant dissociative vibrational excitation by electron impact. The interested reader is referred to Laporta et al. (2015) for a discussion of these precesses.

RVE cross section calculations were performed also for the following process involving the nitric oxide molecule (Laporta et al. 2012b):

$$e+\mathrm{NO}(\mathrm{X}\,^2\Pi, v_i = 0{-}54) \rightarrow \mathrm{NO}^-(^3\Sigma^-,^1\Delta,^1\Sigma^+) \rightarrow e+\mathrm{NO}(\mathrm{X}\,^2\Pi, v_f = 0{-}54). \tag{1.22}$$

which involves three different resonant NO^- states. In this case the potential curves for the resonant and neutral electronic states were expressed as Morse functions optimized to fit the calculated values (Gilmore 1965), while the widths were adjusted in order to reproduce the experimental cross sections (Allan 2005). The obtained potentials and widths are shown in Fig. 1.9. The $\Gamma(R)$ of Fig. 1.9b were found in good agreement with the ab initio results of Trevisan et al. (2005) in the available range of internuclear distances (Laporta et al. 2012b). The cross sections for process (1.22) are shown in Fig. 1.10. The figure shows that the peak position is well reproduced by the theoretical calculations, while some difference is observed in their intensity. However, except for the elastic case, our cross section are on the contrary in very good agreement with the theoretical cross sections of Trevisan et al. (2005), as shown in Fig. 1.11 for the same transitions. Example of RVE cross sections and rate coefficients are shown in Fig. 1.12 for some elastic and inelastic transitions.

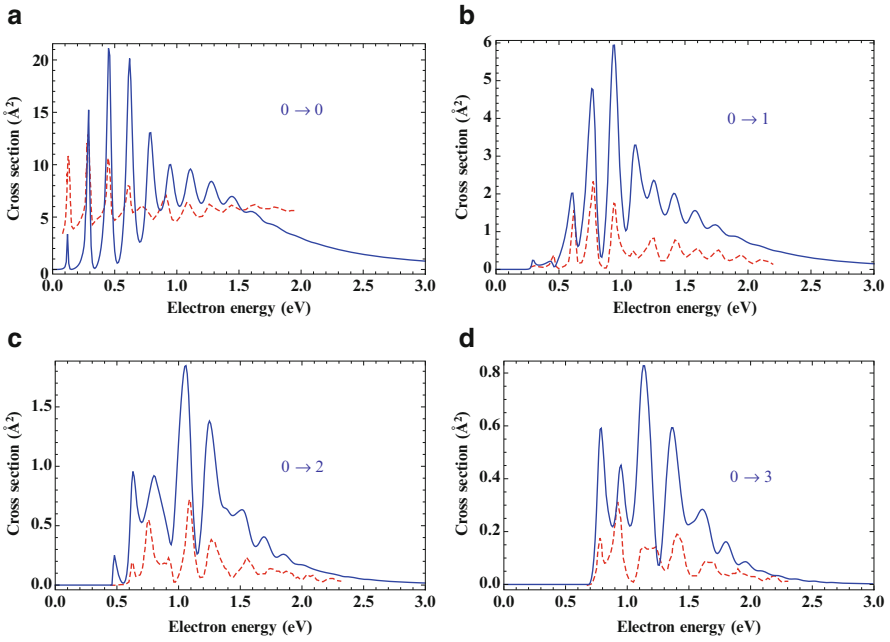

Fig. 1.10 Comparison of the calculated RVE cross sections in *e*-NO collisions (Laporta et al. 2012b) (*solid lines*) with the experiments (Allan 2005) (*dashed lines*) for the transitions shown in the figures

1.2.2 CO *and* CO_2 *Molecules*

RVE cross sections calculations have been extended also to the process (Laporta et al. 2012a)

$$e + \mathrm{CO}(\mathrm{X}\,^1\Sigma^+, v_i = 0 - 80) \rightarrow \mathrm{CO}^-(^2\Pi) \rightarrow e + \mathrm{CO}(\mathrm{X}\,^1\Sigma^+, v_f = 0 - 80)\,, \tag{1.23}$$

which proceeds through the $^2\Pi$ resonant states. Potential energy curves for this state, as well as for $\mathrm{CO}(\mathrm{X}\,^1\Sigma^+)$ state and the resonance width, were calculated ab initio by using MOLPRO and R-matrix method (Laporta et al. 2012a). Figure 1.13 shows the results. In particular in the right panel are represented the calculated points and the analytical fit obtained by assuming for $\Gamma(R)$ the polynomial expression,

$$\Gamma(R) = \left(-302.66 + 635.8R - 480.06R^2 + 156.9R^3 - 18.88R^4\right) \times \\ \times \Theta\left[\mathrm{V}^-(R) - \mathrm{V}_M^0(R)\right](\mathrm{eV}), \tag{1.24}$$